Journal of Power Sources 196 (2011) 7616–7626

Contents lists available at ScienceDirect

Journal of Power Sources

journal homepage: www.elsevier.com/locate/jpowsour

Design and simulation of a liquid electrolyte passive direct methanol fuel cell with low methanol crossover

Weiwei Cai[a,c], Songtao Li[d], Liang Yan[a,c], Ligang Feng[a,c], Jing Zhang[a,c], Liang Liang[a,b], Wei Xing[a,*], Changpeng Liu[b,*]

[a] State Key Laboratory of Electroanalytical Chemistry, Changchun Institute of Applied Chemistry, 5625 Renmin Street, Changchun 130022, PR China
[b] Laboratory of Advanced Power Sources, Changchun Institute of Applied Chemistry, 5625 Renmin Street, Changchun 130022, PR China
[c] Graduate School of the Chinese Academy of Sciences, Beijing, PR China
[d] Mathematics School & Institute, Jilin University, Changchun, PR China

ARTICLE INFO

Article history:
Received 28 February 2011
Received in revised form 30 April 2011
Accepted 6 May 2011
Available online 17 May 2011

Keywords:
Liquid electrolyte
Passive direct methanol fuel cell
Mathematical model
Methanol crossover
Highly concentrated methanol

ABSTRACT

This study investigates an aqueous solution of sulfuric acid that serves as the liquid electrolyte (LE) in a passive direct methanol fuel cell (DMFC). The addition of an LE can reduce methanol crossover and increase the fuel utilization significantly. To improve the performance of an LE-DMFC, a mathematical model is developed to optimize the thicknesses of both the LE layer and the Nafion membrane. The maximum power density of the LE-DMFC is improved by approximately 30% compared with a conventional DMFC (C-DMFC) when each is fed by methanol solutions of the same concentration. Due to the low methanol crossover of the LE-DMFC, a highly concentrated methanol solution can be directly fed into the LE-DMFC. The discharge time and volume energy density of the LE-DMFC are two times longer and three times greater than those of the C-DMFC, respectively. In addition, fuel utilization increases by approximately 100%.

1. Introduction

Direct methanol fuel cells (DMFCs), especially passive DMFCs, are attractive power sources for mobile electric devices because of their features, which include the high specific energy density of methanol, its simple structure and its low operating temperature [1]. However, the issue of high methanol crossover through the proton exchange membrane (PEM) significantly lowers the electrochemical performance and unit power of a DMFC [2]. Many studies have been performed in the field of methanol crossover reduction membranes and modified Nafion membranes to reduce the methanol crossover of DMFC [3–16]. However, none of these membranes can replace the commercial Nafion membrane in a DMFC due to their low proton conductivity and poor stability.

A simple method to reduce the methanol crossover in a DMFC was introduced by Kordesch et al. [17]. A circulating electrolyte layer was used to replace the PEM in the DMFC to form a flowing electrolyte DMFC (FE-DMFC). The open circuit voltage (OCV) of this FE-DMFC pumped with a high concentration of methanol ($10\,mol\,L^{-1}$) remains at approximately 0.8 V. Schaffer et al. [18] designed another FE-DMFC with one Nafion membrane on the anode side. Their results showed that the pumped liquid electrolyte minimized methanol crossover effectively and improved DMFC performance significantly. Mathematical models have also been developed for FE-DMFCs to simulate the effects of different operation conditions on methanol crossover [19,20]. However, all of the reported FE-DMFCs require extra auxiliary equipment (such as a pump for circulating the electrolyte) and consume more energy than conventional DMFCs (C-DMFCs). Therefore, the method of adding a circulating electrolyte layer is not suitable for passive DMFCs because they require a simplified structure.

In this work, we proposed a new design for a passive DMFC with a composite electrolyte to replace the solid PEM in a C-DMFC. Fig. 1a shows the composite electrolyte with two Nafion membranes with a liquid electrolyte (LE) layer in between. The LE layer reduces the methanol crossover in a DMFC because of the different proton transfer mechanisms in the LE and the Nafion membrane, as reported in [21]. Proton transfer in the LE layer follows the Grotthus proton-transfer mechanism, which involves less water and methanol than the vehicle proton-transfer mechanism, which plays a leading role in the Nafion membrane. The thicknesses of the LE layer and the Nafion membrane for the composite electrolyte are optimized by the development of a mathematical model. The electrochemical and discharge performances of the LE-DMFC are also studied through both experiments and calculations.

* Corresponding authors. Tel.: +86 431 85262223; fax: +86 431 85685653.
E-mail addresses: xingwei@ciac.jl.cn (W. Xing), liuchp@ciac.jl.cn (C. Liu).

0378-7753/$ – see front matter © 2011 Elsevier B.V. All rights reserved.
doi:10.1016/j.jpowsour.2011.05.006

Nomenclature

c_1	methanol concentrations in the Nafion/anode electrode interface
c_2	methanol concentrations in the Nafion/LE interface on the anode side
c_3	methanol concentrations in the Nafion/LE interface on the cathode side
c_4	methanol concentrations in the Nafion/cathode electrode interface
c_{in}	methanol concentrations in the fuel reservoir
c_{ac}	methanol concentration in the anode catalyst layer
c_{cc}	oxygen concentration in the cathode catalyst layer
c^a_{ref}	reference methanol concentration on the anode side
c^c_{ref}	reference oxygen concentration on the cathode side
D_w	diffusion coefficient of methanol in water
D_m	diffusion coefficient of methanol in the Nafion membrane
F	Faraday's constant
I	current density of the fuel cell
I_a	current density on the anode side
I_{ct}	total current density on the cathode side
I^a_{ref}	reference exchange current density of the anode
I^c_{ref}	reference exchange current density of cathode
N_{ad}	methanol flux through the anode diffusion layer
N_{le}	methanol crossover flux through the LE layer
N_m	methanol crossover flux through the Nafion membrane
R	universal gas constant
T	cell temperature

Greek letters

α_a	anode transfer coefficient
α_c	cathode transfer coefficient
γ_a	order of anode reaction
γ_c	order of cathode reaction
λ	electro-osmotic drag confident of water
δ_{ac}	thickness of the anode catalyst layer
δ_{ad}	thickness of the anode diffusion layer
δ_{cc}	thickness of the cathode catalyst layer
δ_{cd}	thickness of the cathode diffusion layer
δ_{le}	thickness of the LE layer
δ_m	thickness of the membrane
ε_{ad}	porosity of the anode diffusion layer
η_a	anode overpotential
η_c	cathode overpotential

2. Experiments

2.1. Preparation of the half-MEAs

The sandwich structural MEA in conventional DMFCs was replaced by a composite electrolyte MEA in the LE-DMFC. The composite electrolyte MEA consisted of a LE layer between two half-MEAs. The half-MEA contained a catalyst layer (CL), a diffusion layer (DL) and a Nafion membrane.

PtRu/C (20 wt.% Pt, Pt:Ru = 1:1) powder and Pt/C (20 wt.% Pt) powder were suspended in Nafion solution containing 10% PTFE under ultrasonic conditions until a homogeneous ink was formed. The ink was sprayed to 20% PTFE wet-proofed carbon paper and cured at 340 °C in a nitrogen-filled vacuum oven for 1 h to form the anode and cathode electrodes. The Pt and Nafion loadings in both catalyst layers were approximately 2 mg cm^{-2} and 1 mg cm^{-2}, respectively. The anode and cathode electrodes were hot-pressed to the membranes at 130 °C and 100 MPa for 3 min to obtain two half-MEAs for the anode and cathode.

2.2. LE-DMFC fabrication

Piled hydrophilic filter papers acted as the carrier for the LE. The thickness of the LE layer was determined by the number of paper piles. The two half-MEAs prepared as described in Section 2.1 were then assembled with the LE layer to obtain the composite electrolyte MEA, as shown in Fig. 1b. The composite electrolyte MEA was immobilized within the fuel reservoir, current collectors, and gaskets by the screws to obtain the LE-DMFC.

2.3. Electrochemical studies

After the composite MEA was installed in the cell, a methanol solution was injected into the fuel reservoir at room temperature (25 °C). The polarization and discharge curves of the conventional DMFC and LE-DMFC were compared.

3. Mathematical model

For the passive DMFC, the temperature difference inside the cell was very small (<0.15 °C) during operation [22]. This temperature difference was negligible compared with the DMFC operating temperature; therefore, thermal transfer equations were not considered is this model. In other words, in this study, we proposed an isothermal mathematical model containing mass transfer and potential equations.

In the liquid electrolyte, hydrated water molecules did not transfer together with the protons in the Nafion membrane during the operation process of the LE-DMFC. Therefore, the use of an LE layer in the LEDMFC significantly decreased the permeating rate of water from the anode to the cathode side. The methanol crossover flux was also reduced due to the intersolubility of methanol and water. Four methanol concentrations, which are symbolized as c_1–c_4, were used in the mathematical model, as shown in Fig. 1a. These four characteristic concentrations represented the concentration distribution of methanol across the composite electrolyte. c_1 and c_4 corresponded to the methanol concentrations in the Nafion/electrode interfaces of the anode and cathode sides, respectively, and c_2 and c_3 corresponded to the methanol concentrations in the Nafion/LE interfaces of the anode and cathode sides, respectively. c_4 was set at zero for the calculation. Therefore, the methanol crossover fluxes through the two PEMs can be calculated by the following two equations:

$$N_{m1} = \frac{D_m}{\delta_{m1}}(c_1 - c_2) + \frac{18\lambda I}{F}c_1 \quad (1)$$

$$N_{m2} = \frac{D_m}{\delta_{m2}}c_3 + \frac{18\lambda I}{F}c_3 \quad (2)$$

In both Eqs. (1) and (2), the first term on the right side represents the diffusion methanol across the Nafion membrane, and the second term is the electro-osmotic drag. The subscripts $m1$ and $m2$ correspond to the Nafion membrane on the anode and cathode sides, respectively. F is Faraday's constant, and δ_m is the thickness of Nafion membrane. D_m and λ are methanol diffusivity and the electro-osmotic drag coefficient of water in Nafion membrane, respectively. I is the operation current density of the DMFC.

The methanol permeation flux across the LE layer can be described by Fick's law

$$N_{le} = \frac{D_w}{\delta_{le}}(c_2 - c_3) \quad (3)$$

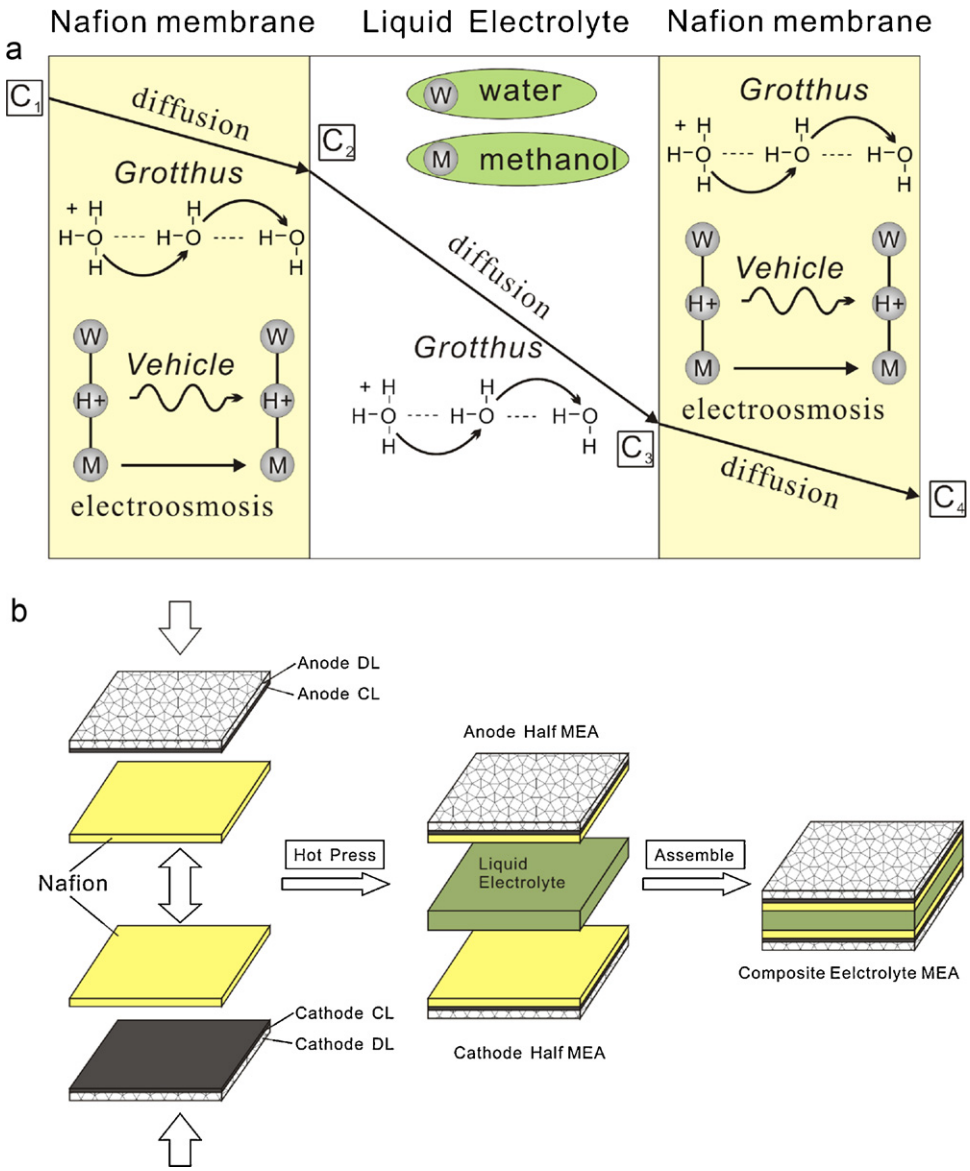

Fig. 1. (a) Schematic diagram of methanol permeation through the composite electrolyte; (b) fabrication of composite electrolyte MEA for LE-DMFC.

where D_w is the methanol diffusivity in aqueous solution and δ_{le} is the thickness of the LE layer.

The previously mentioned methanol permeation fluxes N_{m1}, N_{m2} and N_{le} were equivalent to each other because no methanol was consumed by the composite electrolyte. Therefore, we can combine Eqs. (2) and (3) to obtain the relationship between the methanol concentrations c_2 and c_3

$$\frac{D_w}{\delta_{le}}c_2 = \left(\frac{D_w}{\delta_2} + \frac{D_m}{\delta_m} + \frac{18\lambda I}{F}\right)c_3 \Rightarrow \frac{D_w/\delta_{le}}{D_w/\delta_{le} + D_m/\delta_m + 18\lambda I/F}c_2 = c_3 \quad (4)$$

Given Eq. (1), the relationship between c_1 and c_3 can be expressed as follows

$$c_1 = \left[\left(\frac{D_w}{\delta_{le}} + \frac{D_m}{\delta_m}\right)\frac{D_w/\delta_{le} + D_m/\delta_m + 18\lambda I/F}{D_w/\delta_{le}} - \left(\frac{D_w}{\delta_{le}}\right)\right] \times \frac{c_3}{(D_m/\delta_m) + (18\lambda I/F)} \quad (5)$$

To calculate the three characteristic methanol concentrations c_1, c_2, and c_3, the relationship between methanol concentration c_1 and methanol permeation flux through the anode diffusion layer N_{ad} is expressed below as

$$N_{ad} = \frac{\varepsilon_{ad}^{1.5} D_w}{\delta_{ad}}(c_{in} - c_1) \quad (6)$$

where the factor 1.5 is the Bruggemann correction coefficient [23] for porous systems; ε_{ad} and δ_{ad} are the porosity and thickness of the anode diffusion layer, respectively; and c_{in} is the methanol concentration in the fuel reservoir of the LE-DMFC.

Methanol that was transferred through the anode diffusion layer reacted in the anode catalyst layer with water according to the following equation

$$CH_3OH + H_2O \rightarrow CO_2 + 6H^+ + 6e^- \quad (7)$$

In the LE-DMFC, the residual methanol transferred across the composite electrolyte to the cathode side, and the crossover flux was N_{m2}. This gives the following equilibrium equation

$$N_{ad} = \frac{I}{6F} + N_{m2} \quad (8)$$

By combining Eq. (8) with (4) and (5), the methanol concentrations c_1, c_2, and c_3 can be calculated.

The Butler–Volmer equation is employed in this model to calculate the anode and cathode overpotential,

$$I_a = I^a_{ref}\left(\frac{c_{ac}}{c^a_{ref}}\right)^{\gamma_a} \exp\left(\frac{\alpha_a F}{RT}\eta_a\right) \quad (9)$$

$$I_{ct} = I^c_{ref}\left(\frac{c_{cc}}{c^c_{ref}}\right)^{\gamma_c} \exp\left(\frac{\alpha_c F}{RT}\eta_c\right) \quad (10)$$

The current density in the anode side I_a was equivalent to the cell operating current density I. The permeated methanol in the cathode catalyst layer was believed to react completely with oxygen through an electro-oxidation reaction; therefore, the total current density on the cathode side I_{ct} was defined as $I_{ct} = I + 6FN_m$. In Eq. (9), c_{ac} represents the methanol concentration in the anode catalyst layer, and its value was considered to be equivalent to c_1. In Eq. (10), c_{cc} is the oxygen concentration in the cathode catalyst layer. The definition of every symbol in the above-mentioned equations is given in the nomenclature list, and the values of the parameters are illustrated in Table 1.

4. Results and discussion

4.1. Optimization of LE thickness

The effect of LE thickness on fuel cell performance was studied using a mathematical model. The concentration of the LE was kept constant (1.0 mol L^{-1} sulfuric acid). Fig. 2 shows the relationship between the calculated cell voltage and the LE thickness of the LE-

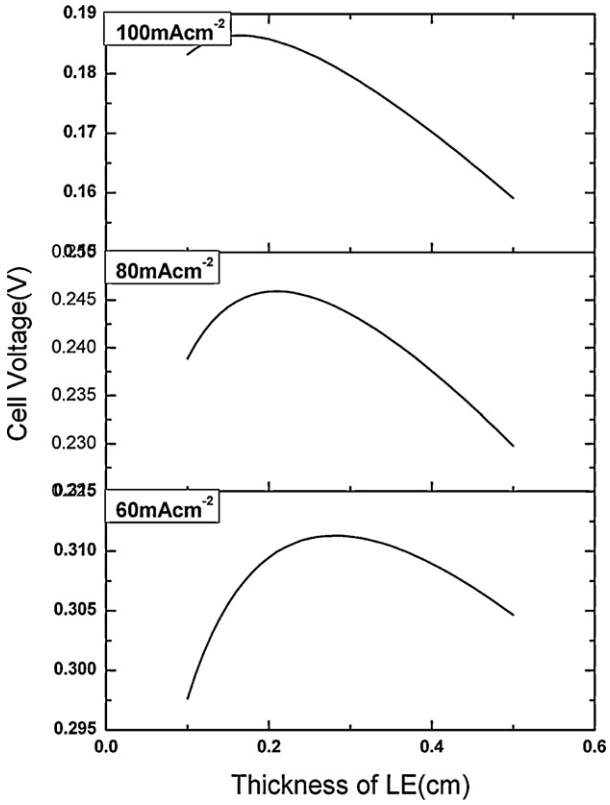

Fig. 2. Dependence of cell voltage on liquid electrolyte thickness calculated from the model.

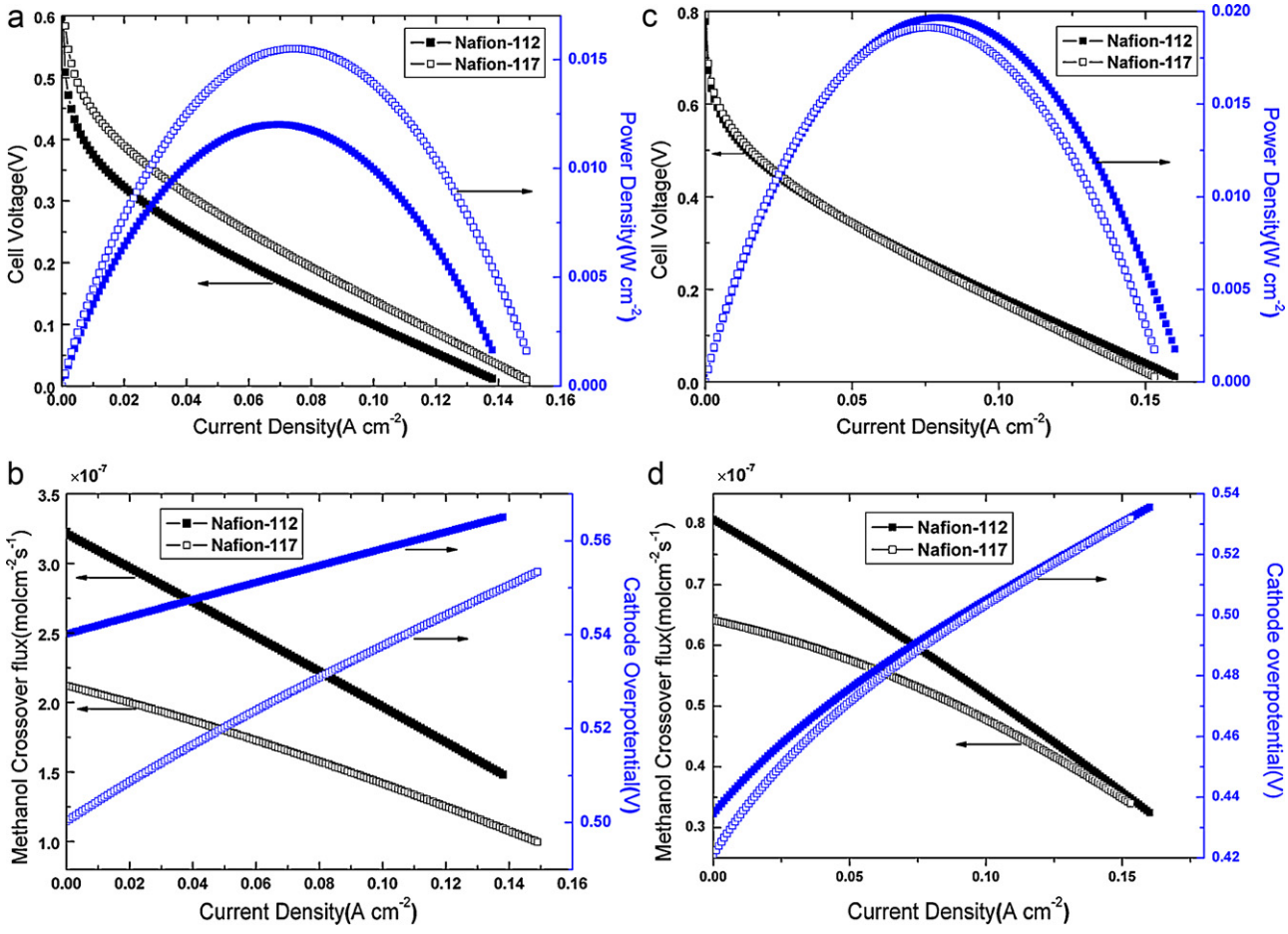

Fig. 3. Comparisons of calculated (a) polarization data; (b) methanol crossover flux and cathode overpotential of a C-DMFC using Nafion 112 and 117. (c) Polarization data; (d) methanol crossover flux and cathode overpotential of a LE-DMFC using Nafion 112 and 117.

Table 1
Parameter values.

Parameter/symbol (unit)	Value	Ref.
Cell temperature/T (K)	298.15	
Reference methanol concentration/c^a_{ref} (mol cm^{-3})	1×10^{-3}	[24]
Reference oxygen concentration/c^c_{ref}(mol cm^{-3})	$1 \times 10^{-6} \times 101{,}325/(RT)$	[24]
Diffusion coefficient of methanol in water/D_w (cm^2 s^{-1})	$2.8 \times 10^{-6} \exp\left(\frac{2436}{353} - \frac{2436}{T}\right)$	[24]
Diffusion coefficient of methanol in membrane/D_m (cm^2 s^{-1})	$4.9 \times 10^{-6} \exp\left(\frac{2436}{333} - \frac{2436}{T}\right)$	[24]
Faraday's constant/F	96,487	
Reference exchange current density of anode/I^a_{ref} (A cm^{-2})	$0.011 \times \delta_{ac}$	[25]
Thickness of cathode catalyst layer/δ_{ac} (cm)	0.005	Assumed
Reference exchange current density of cathode/j^c_{ref} (A cm^{-2})	$0.011 \times \delta_{cc}$	[25]
Thickness of cathode catalyst layer/δ_{cc} (cm)	0.005	Assumed
Electro-osmotic drag coefficient of water/λ	$2.9 \exp\left(\frac{1029}{333} - \frac{1029}{T}\right)$	[26]
Contact resistance of cell/R_{con} (Ω cm^2)	1.2	Assumed
Conductivity of Nafion membrane/σ_m (S cm^{-1})	$0.073 \exp\left(1268\left(\frac{1}{298} - \frac{1}{T}\right)\right)$	[24]
Order of anode reaction/γ_a	1	Assumed
Order of cathode reaction/γ_c	1	Assumed
Anodic transfer coefficient/α_a	0.5	Assumed
Cathodic transfer coefficient/α_c	0.5	Assumed
Thickness of anode diffusion layer/δ_{ad} (cm)	0.003	
Thickness of cathode diffusion layer/δ_{cd} (cm)	0.003	

DMFC when loading different operating current densities with a 3.0 mol L^{-1} methanol solution. We investigated an LE layer with a thickness range of 0.1–0.5 cm at current densities set at 60, 80, and 100 mA cm^{-2}. The cell voltage apparently depended on the LE thickness at these three current densities. When 60 mA cm^{-2} was used, the cell voltage reached its peak value when the LE thickness was approximately 0.26 cm. As the current densities increased to 80 and 100 mA cm^{-2}, the optimal thickness of the LE decreased to 0.22 cm and 0.16 cm, respectively. A LE layer with 0.2 cm thickness was chosen for further investigation.

4.2. Effect of PEM thickness

The thickness of the PEM can strongly affect the methanol crossover flux of the DMFC. Therefore, Nafion membranes with different thickness were used for both the C-DMFC and the LE-DMFC in this mathematical model.

Calculated polarization data for the C-DMFCs, which were assembled with Nafion 112 (C-DMFC-112) and Nafion 117 (C-DMFC-117) membranes are shown in Fig. 3a, and 3.0 mol L^{-1} methanol solution was used. The cell voltage of the C-DMFC-117 during the polarization process was much greater than that of the C-DMFC-112. The maximum power density of the C-DMFC-117 was approximately 15.5 mW cm^{-2}, which was 29% higher than that of the C-DMFC-112. The better electrochemical performance of the C-DMFC-117 was due to its lower methanol crossover flux compared with the C-DMFC-112 as shown in Fig. 3b, which can be attributed to the thicker PEM. Lower methanol crossover resulted in a cathode overpotential for C-DMFC-117 that was 30 mV lower than that of C-DMFC-112.

Fig. 3c shows the comparisons of LE-DMFC performances using Nafion 112 and Nafion 117 as the PEM. We used a 0.2-cm thick LE layer with the LE-DMFC for the calculations. When a 3.0 mol L^{-1} methanol concentration was used, the calculated polarization curves for LE-DMFC-117 LE-DMFC-112 were almost identical to those shown in Fig. 3c. The maximum power density of the LE-DMFC-112 was approximately 3% higher than that of LE-DMFC-117. In addition, the methanol crossover fluxes and cathode overpotentials of these two LE-DMFCs were slightly different, as shown in Fig. 3d. Therefore, the lower proton transfer resistance of the LE-DMFC-112 caused by the minimal thickness of the PEM was the main reason that it had a better electrochemical performance than the LE-DMFC-117.

Fig. 4 shows another comparison between the cell performances of the C-DMFC-117 and the LE-DMFC-112 supplied with a 3.0 mol L^{-1} methanol solution. The LE-DMFC performed much better than the C-DMFC under these conditions, and the maximum power density of LE-DMFC reached 19.67 mW cm^{-2}, which was approximately 27% higher than that of the C-DMFC.

The better cell performance of the LE-DMFC can be attributed to its lower cathode and anode overpotential compared with the C-DMFC, as shown in Fig. 5a and b. The lower cathode overpotential of the LE-DMFC was caused by its lower methanol crossover flux, as shown in Fig. 5c. The methanol crossover fluxes for both the C-DMFC and the LE-DMFC decreased as current density increased, and the decreasing velocity of the LE-DMFC was much lower. This is because the proton transfer in the LE layer followed the Grotthus mechanism, and the electro-osmotic drag of the methanol crossover flux did not exist in the LE layer during the operation process.In contrast with the C-DMFC, the LE-DMFC also possessed a lower anode overpotential, as shown in Fig. 5b, which was caused by the higher methanol concentration in the anode catalyst layer, as shown in Fig. 5d. The methanol permeating across the anode diffusion layer was consumed in two ways, through electro-oxidation on the anode side and by crossover to the cathode side. The methanol reaction velocities in the anode CL of the LE-DMFC and the C-DMFC

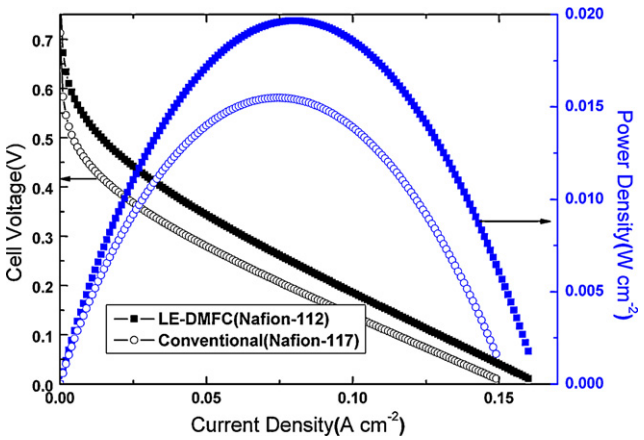

Fig. 4. Comparison of calculated electrochemical performance of a LE-DMFC with a C-DMFC. (3.0 mol L^{-1} methanol solution).

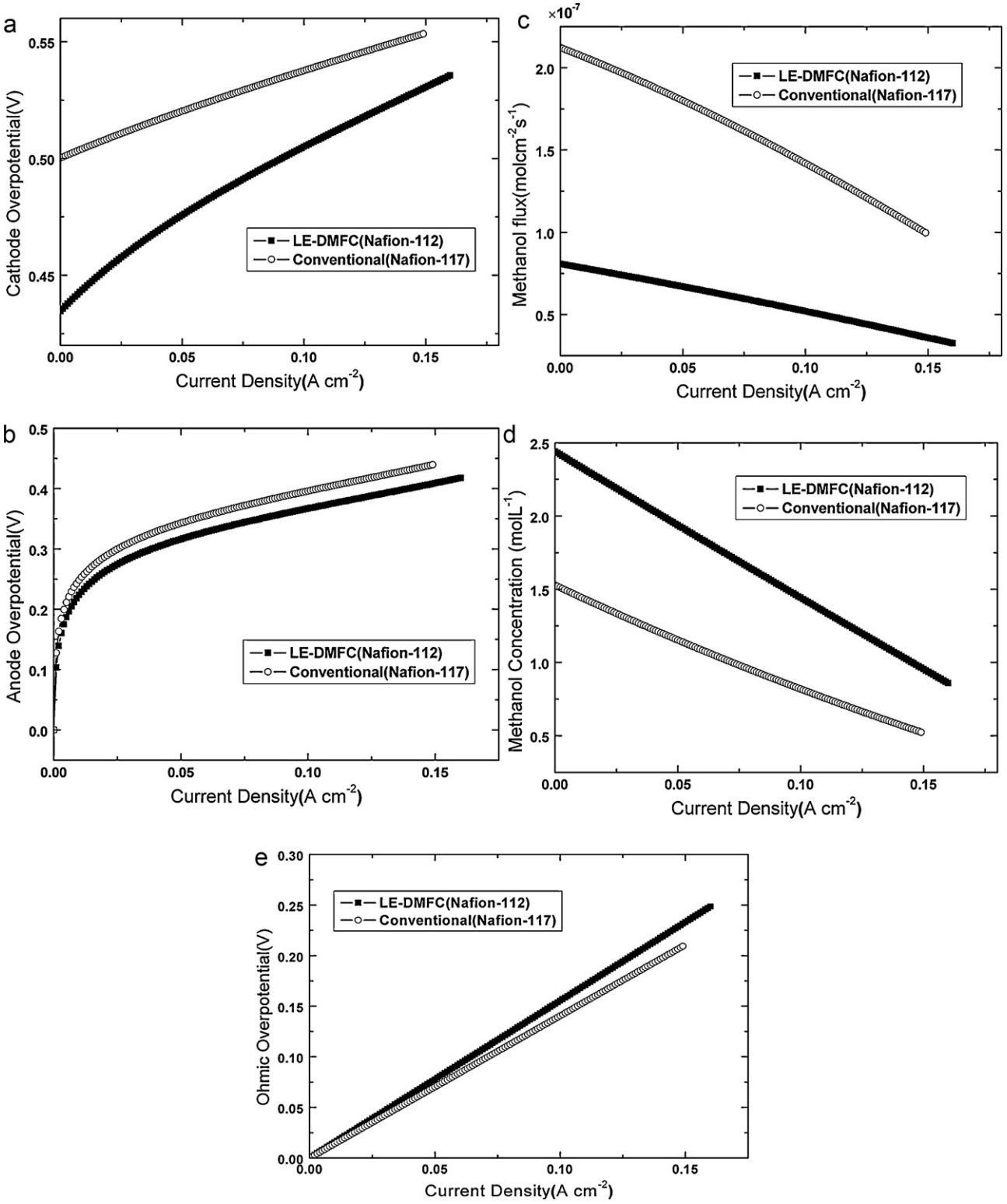

Fig. 5. Comparison of calculated (a) cathode overpotential; (b) anode overpotential; (c) methanol crossover flux; (d) methanol concentration in anode CL; (e) ohmic overpotential of a LE-DMFC with a C-DMFC (3.0 mol L^{-1} methanol solution).

were equivalent at the same current density. Therefore, the lower methanol crossover flux of the LE-DMFC spontaneously resulted in a higher methanol concentration in the anode CL of the LE-DMFC.

Fig. 5e compares the ohmic overpotential variations for the LE-DMFC and the C-DMFC with current density. For both of the DMFCs, the ohmic overpotential was linear with the current density because the resistance of the DMFC did not vary with the current density. The ohmic overpotential difference between the LE-DMFC and the C-DMFC was negligible when the current density was small. When the current density increased to 100 mA cm^{-2},

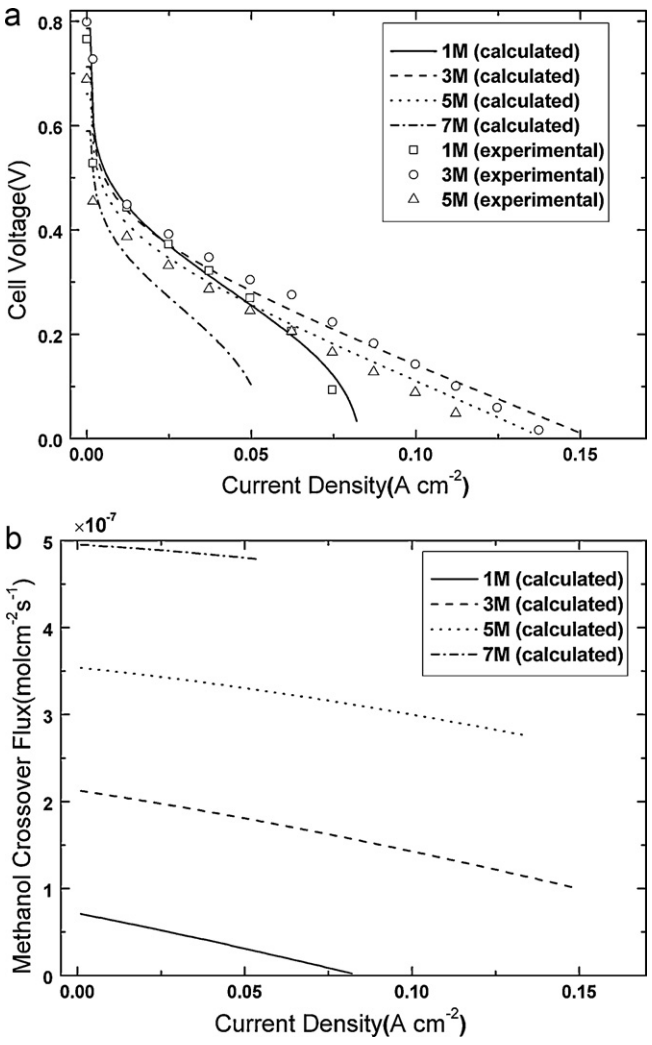

Fig. 6. (a) Calculated and experimental polarization data; (b) calculated methanol crossover flux data of a C-DMFC with different methanol concentrations.

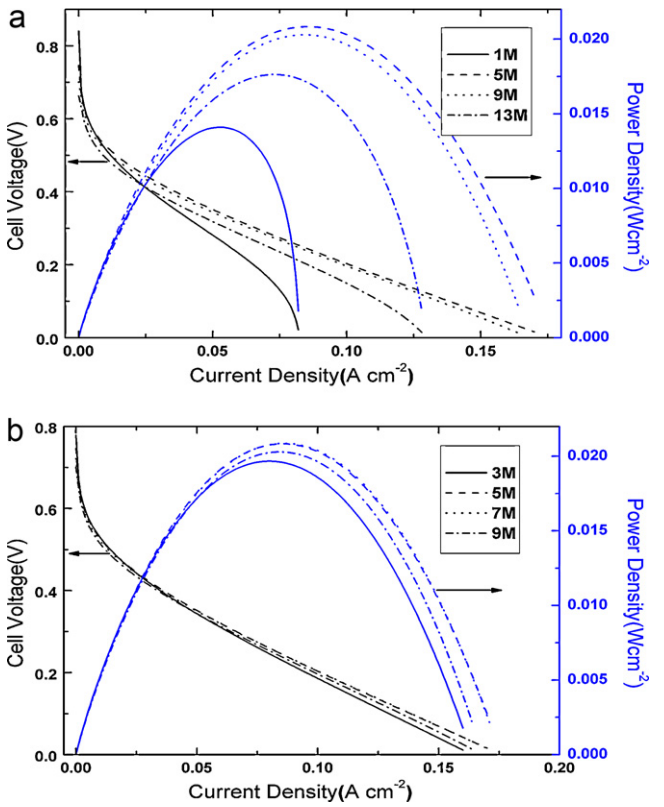

Fig. 7. Polarization curves for the LE-DMFC with different methanol concentrations.

the ohmic overpotential of the LE-DMFC was only approximately 15 mV greater than that of the C-DMFC.

Given the above-mentioned information, we concluded that the thinner Nafion 112 membrane was more suitable for the LE-DMFC than the Nafion 117, which is commonly used as a PEM in C-DMFCs. In addition, the LE-DMFC showed much better performance than the C-DMFC.

4.3. Effect of methanol concentration

The calculated and experimental polarization results of a C-DMFC supplied with differing concentrations of methanol solutions are shown in Fig. 6a. The calculated results illustrate that the C-DMFC had the best electrochemical performance when it was fed with a 3.0 mol L^{-1} methanol solution. Any increase of methanol concentration above 3.0 mol L^{-1} caused a rapid degradation of performance, and the cell voltage of a C-DMFC fed with a 7.0 mol L^{-1} methanol solution was even lower than that fed with 1.0 mol L^{-1}. This was due to the dependence of the methanol crossover flux on the feeding methanol concentration, as shown in Fig. 6b. The value of the methanol crossover flux with 7.0 mol L^{-1} was more than five times greater than the flux with 1.0 mol L^{-1}. Fig. 6a also shows the experimental polarization data for the C-DMFC with methanol solutions ranging from 1.0 to 5.0 mol L^{-1} to validate the mathematical model. The results showed that the analytical results agreed quite well with the experimental data for all three concentrations.

Section 4.2 proved that the LE-DMFC had a lower methanol crossover flux than the C-DMFC. Therefore, it is reasonable to supply a highly concentrated methanol solution into the fuel reservoir of an LE-DMFC. Fig. 7 shows the calculated polarization data for the LE-DMFC fed with differing concentration methanol solutions. Methanol concentrations ranging from 1.0 mol L^{-1} to 13.0 mol L^{-1} were investigated by running the mathematical model for the LE-DMFC, and the results are shown in Fig. 7a. The LE-DMFC that was supplied with a 1.0 mol L^{-1} methanol solution exhibited the worst electrochemical performance, and the maximum power density in this case was only 14.10 mW cm^{-2}. The cell voltage of the LE-DMFC increased as the feeding methanol concentration increased, and the best electrochemical performance for the LE-DMFC occurred when it was fed with a 5.0 mol L^{-1} methanol solution. The maximum power density of the LE-DMFC fed with a 5.0 mol L^{-1} methanol solution was approximately 50% higher than that of the 1.0 mol L^{-1} solution. An increase of the methanol concentration over 5.0 mol L^{-1} caused a very small decrease in the cell performance. When the feeding methanol concentration increased to 13.0 mol L^{-1}, the LE-DMFC still performed much better than the LE-DMFC that was fed with 1.0 mol L^{-1} methanol solution. A comparison of the polarization data for the LE-DMFC with 3.0–9.0 mol L^{-1} methanol solution is shown in Fig. 7b. The polarization curves of 5.0 mol L^{-1} and 7.0 mol L^{-1} were identical, and the cell performances of the LE-DMFC with 3.0 mol L^{-1} and 9.0 mol L^{-1} methanol solutions were slightly lower. The calculated results verified that the LE-DMFC can be supplied with highly concentrated methanol.

A methanol solution of 3.0 mol L^{-1} is the most commonly used fuel for passive C-DMFCs, and 12.0 mol L^{-1} is considered to be a

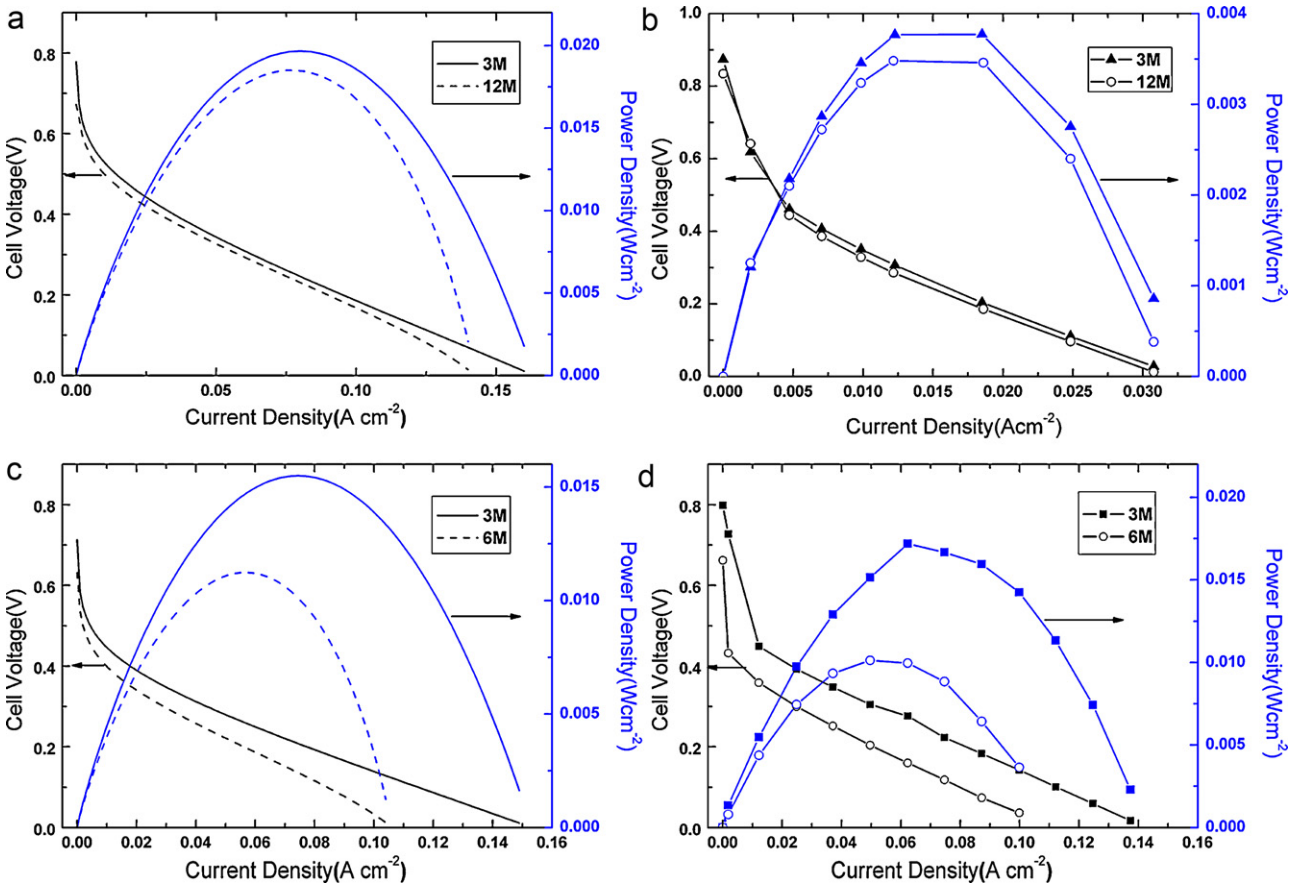

Fig. 8. Comparison of (a) calculated polarization data for LE-DMFC; (b) experimental polarization data for LE-DMFC; (c) calculated polarization data for C-DMFC; (d) experimental polarization data for C-DMFC with high and common-used methanol concentration.

very high concentration because the volume ratio of methanol-to-water in this concentration is approximately 1:1. Therefore, the performance of the LE-DMFC was compared under conditions of 3.0 mol L^{-1} and 12.0 mol L^{-1} methanol solutions. Fig. 8a and b shows the calculated and experimental polarization data for the LE-DMFC, respectively. The calculated results show that performance of the LE-DMFC that was fed with 3.0 mol L^{-1} methanol solution was slightly better than the case of 12.0 mol L^{-1}. The maximum power densities for these two cases only differed by 6%. The cell voltages of the experimental results were much lower than the predicted data calculated from the proposed model, as shown in Fig. 8b, because the actual contact resistance (total resistance: 2.4 Ω for the LE-DMFC with 4 cm^2 active surface area) was much higher than expected (0.3 Ω for a 4 cm^2 electrode). When fed with 3.0 mol L^{-1} and 12.0 mol L^{-1} methanol solutions, the experimental polarization results of LE-DMFC did not differ greatly, which agreed well with the predicted tendency. The maximum power density of the LE-DMFC with 3.0 mol L^{-1} methanol solution was approximately 8% higher than that fed with 12.0 mol L^{-1} methanol solution. In addition, Fig. 8c and d shows the electrochemical performance comparison of the C-DMFC with 3.0 and 6.0 mol L^{-1} methanol solutions. The calculated and experimental results both showed that when 6.0 mol L^{-1} methanol solution was fed into the C-DMFC, the cell performance dramatically declined compared to the one with 3.0 mol L^{-1}. The maximum power density of the C-DMFC supplied with 6.0 mol L^{-1} methanol solution was approximately 70% less than that in 3.0 mol L^{-1} case. In summary, it can be concluded that the LE-DMFC can be supplied with a much more highly concentrated methanol solution than the C-DMFC.

We also performed a two-parameter optimization for the LE-DMFC. Fig. 9 shows cell voltage as a function of feeding methanol concentration and LE thickness (from 0.1 cm to 0.5 cm) at different densities of 40, 60, and 80 mA cm^{-2}. The PEM thickness was set at 0.005 cm. The results in Figs. 9a–c indicate that cell voltage strongly depended on the methanol concentration, whereas the dependence of cell voltage on LE thickness was not evident. The optimal LE thickness changed from 0.1 to 0.5 cm as methanol concentration increased from 1 to 15 mol L^{-1}. More importantly, 6–10 mol L^{-1} were found to be the optimal methanol concentrations according to the two-parameter optimization at any current density. Therefore, the conclusion that the LE-DMFC can be supplied with a highly concentrated methanol solution was valid for all of the investigated LE thickness and current densities.

4.4. Discharging performance

Because the LE-DMFC can be directly supplied with highly concentrated methanol, we must also discuss the discharging performance of the LE-DMFC. The reservoirs of both the LE-DMFC and the C-DMFC had a depth of 2.0 cm, and the cross-area of the reservoirs was equal to the active area of the electrode. Fig. 10 shows the calculated discharging curves of a C-DMFC and a LE-DMFC with various methanol concentrations at 60 mA cm^{-2}. As shown in Fig. 10a, the C-DMFC can work continuously for approximately 12 h when it

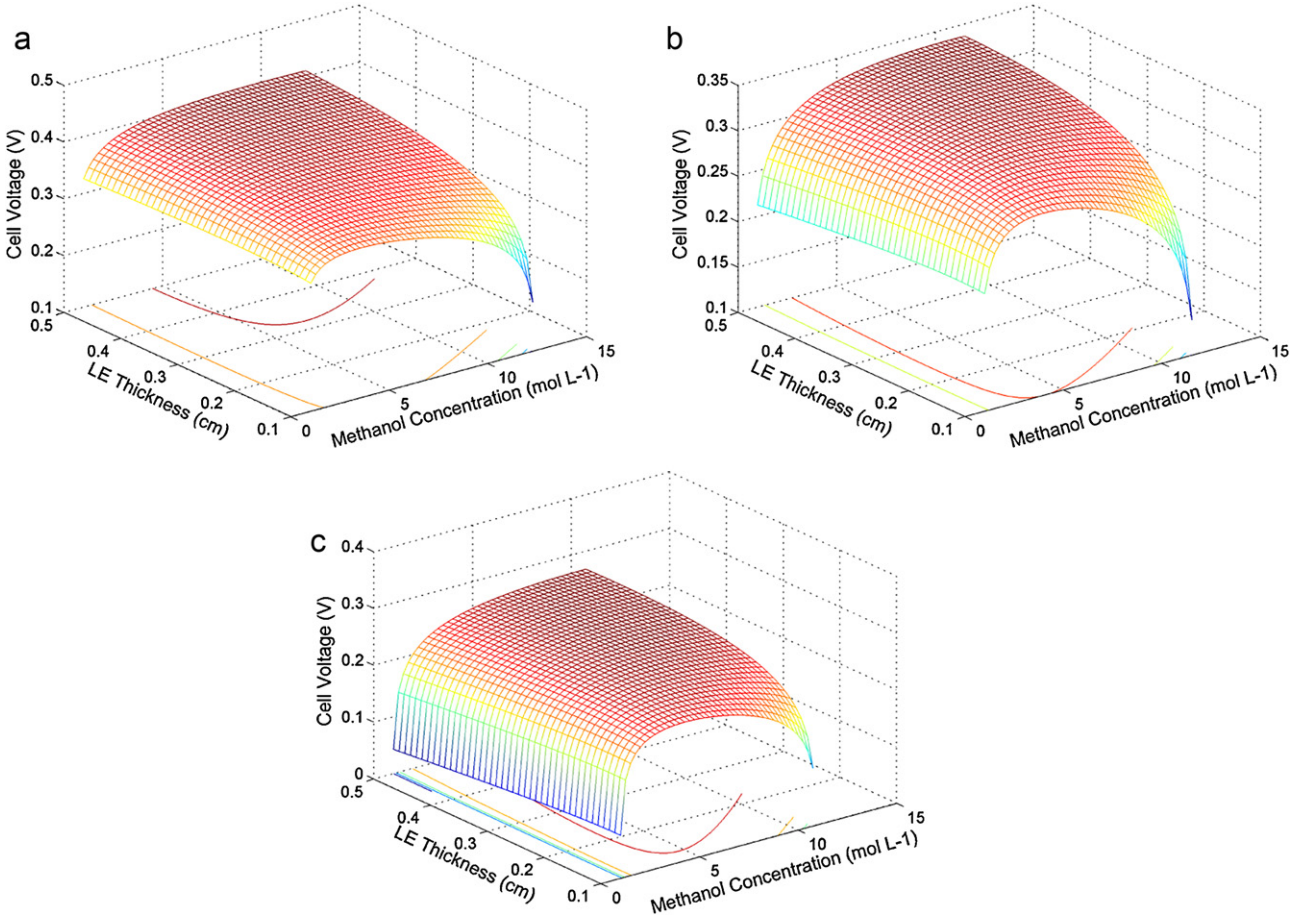

Fig. 9. Cell voltage as a function of feeding methanol concentration and LE thickness at (a) 40 mA cm^{-2}; (b) 60 mA cm^{-2}; (c) 80 mA cm^{-2}.

was supplied with 6.0 mol L^{-1} methanol solution, which is the most concentrated methanol solution that is suitable for the C-DMFC at 60 mA cm^{-2}. The onset voltage for the C-DMFC decreased evidently as the methanol concentration increased from 3.0 mol L^{-1} to 6.0 mol L^{-1}. For comparison, Fig. 10b shows the calculated discharging curves of a LE-DMFC that was supplied with methanol solutions ranging from 3.0 mol L^{-1} to 15.0 mol L^{-1}. The LE-DMFC with 15.0 mol L^{-1} methanol solution could work continuously for approximately 33 h, which was approximately two times longer than the longest discharging time of the C-DMFC.

The LE-DMFC not only had a much longer discharge time than the C-DMFC but also had a much higher cell voltage during the discharging process, as shown in Table 2. The average cell voltages of the C-DMFC that was supplied with 3.0–6.0 mol L^{-1} methanol solutions were all approximately 0.25 V, whereas the average voltages of the LE-DMFC were all larger than 0.29 V. The higher cell voltage during the discharging process for the LE-DMFC was caused by its lower methanol crossover flux than the C-DMFC as discussed in the previous two sections. The average methanol crossover fluxes ($F_{m,av}$) for both the C-DMFC and the LE-DMFC with different concentrations of methanol solutions were calculated and shown in Fig. 10c. When supplying 3.0 mol L^{-1} methanol solution, the $F_{m,av}$ of the C-DMFC was approximately 0.75×10^{-7} mol cm^{-2} s^{-1}, which was approximately two times greater than that of the LE-DMFC. When the methanol concentration increased, the $F_{m,av}$ of the C-DMFC increased much more rapidly than that of the LE-DMC. When supplied with 5.0 mol L^{-1} methanol solution, the average methanol crossover flux of the C-DMFC was approximately 1.25×10^{-7} mol cm^{-2} s^{-1}, which was equivalent to that of the LE-DMFC that was supplied with 15.0 mol L^{-1} methanol solution.

We also compared the energy density and power density of the LE-DMFC and the C-DMFC. Table 3 shows the structural parameters for these two DMFCs. The active area of the electrode for both the C-DMFC and the LE-DMFC was 2 cm × 2 cm. The C-DMFC had a total thickness of 2.3 cm after we packed the MEA, gaskets, current collectors, and the fuel reservoir in series. The LE-DMFC was 0.2 cm thicker than the C-DMFC due to the existence of a LE layer. The cross area of the two fuel cells was 3 cm × 3 cm considering the 0.5 cm width of the reservoir wall.

Fig. 11 shows the calculated energy densities and the average power densities during the discharging process for the C-DMFC and the LE-DMFC with various concentrations of methanol solutions. The energy densities of the DMFCs both increased obviously along with the methanol concentration because a higher methanol concentration caused a longer discharging time, as shown in Fig. 10c. When fed with 5.0 mol L^{-1} methanol solution, the C-DMFC reached its highest energy density at approximately 30 Wh L^{-1}, which was approximately 40% smaller than that of the LE-DMFC under identical working conditions. When fed with 15.0 mol L^{-1} methanol solution, the energy density of the LE-DMFC was approximately 110 Wh L^{-1}. The average power densities for both the LE-DMFC and the C-DMFC supplied with different concentrations of methanol solutions are also compared in Fig. 11. When fed with 13.0 mol L^{-1} methanol solution, the LE-DMFC showed its highest power density of approximately 19.5 mW cm^{-2}, whereas the high-

Table 2
Average cell voltages for C-DMFC and LE-DMFC with different methanol concentrations.

	c_m (mol L^{-1})								
	3.0	4.0	5.0	6.0	7.0	9.0	11.0	13.0	15.0
Average voltage for C-DMFC (V)	0.251	0.255	0.255	0.252					
Average voltage for LE-DMFC (V)	0.290		0.308		0.316	0.321	0.322	0.323	0.322

est power density for the C-DMFC was only approximately 15 mW cm^{-2}.

We also compared the experimental discharging performance of the C-DMFC and the LE-DMFC under identical working conditions. Fig. 12a shows a comparison of the experimental discharging curves of the DMFCs fed with 1.0 mol L^{-1} methanol solution at 2.5 mA cm^{-2}. The structure parameters of the DMFCs were the same as those used in the mathematical model given in Table 3. The C-DMFC could work continuously for 23 h, whereas the discharging time for the LE-DMFC was 48 h. The fuel utilization can be calculated using the following equation

$$\mu = \frac{It/6F}{c_{m,0} l_r} \tag{11}$$

Table 3
Structure parameters for C-DMFC and LE-DMFC used in energy and power output calculation.

	C-DMFC	LE-DMFC
Volume of the fuel cell	3 cm × 3 cm × 2.3 cm	3 cm × 3 cm × 2.5 cm
Volume of the fuel reservoir	2 cm × 2 cm × 2 cm	2 cm × 2 cm × 2 cm
Active area of electrode	2 cm × 2 cm	2 cm × 2 cm

where l_r is the thickness of the fuel reservoir. The fuel utilization of the C-DMFC and the LE-DMFC were 17.88% and 37.31%, respectively. As shown in Fig. 12b, the calculated discharging times for the C-DMFC and the LE-DMFC were 22 and 47 h, which agreed well with the experimental measured data.

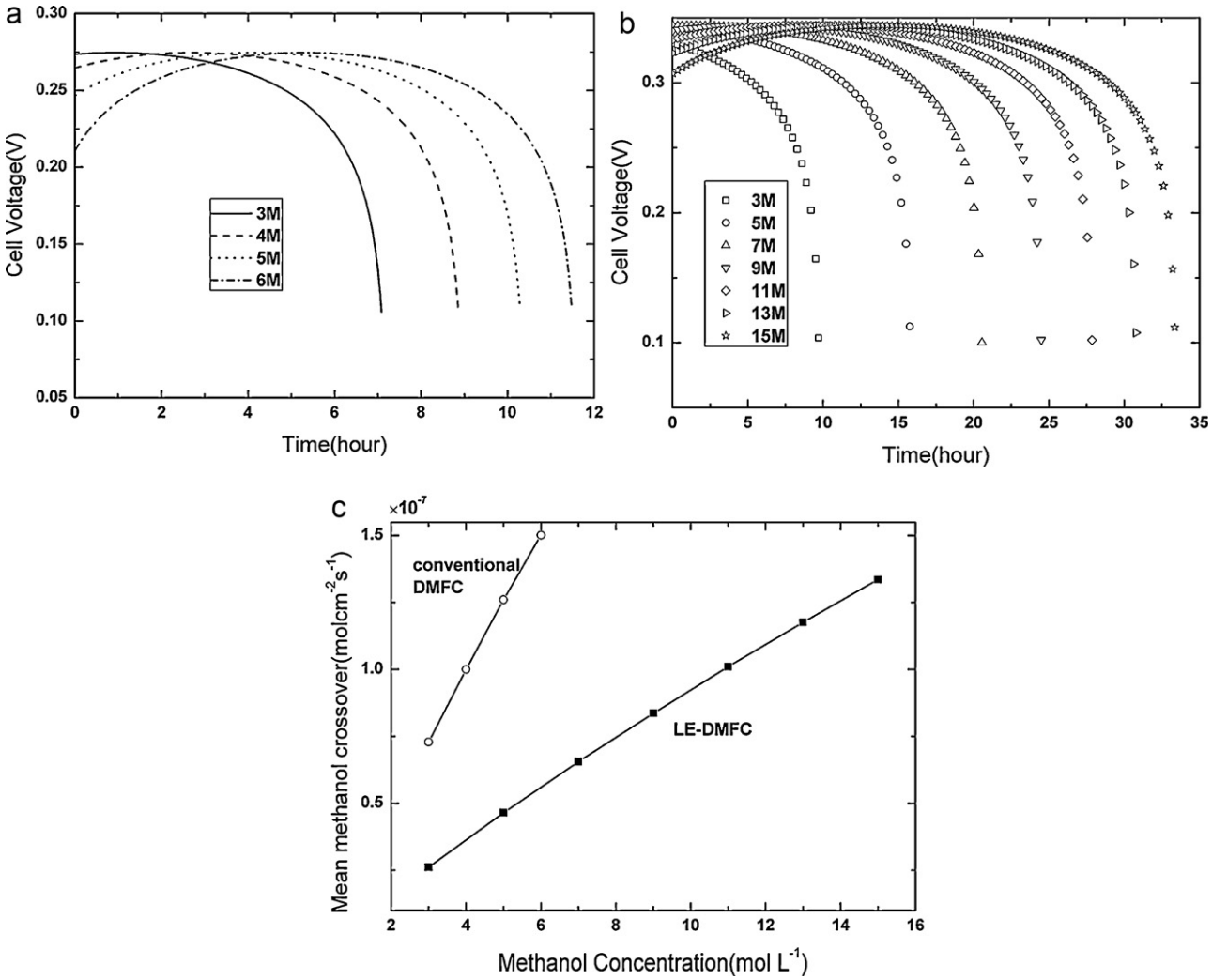

Fig. 10. Calculated discharge curves of (a) a C-DMFC; and (b) a LE-DMFC with various methanol concentrations at 60 mA cm^{-2}. (c) Variations of calculated average methanol crossover flux with methanol concentrations for C-DMFC and LE-DMFC.

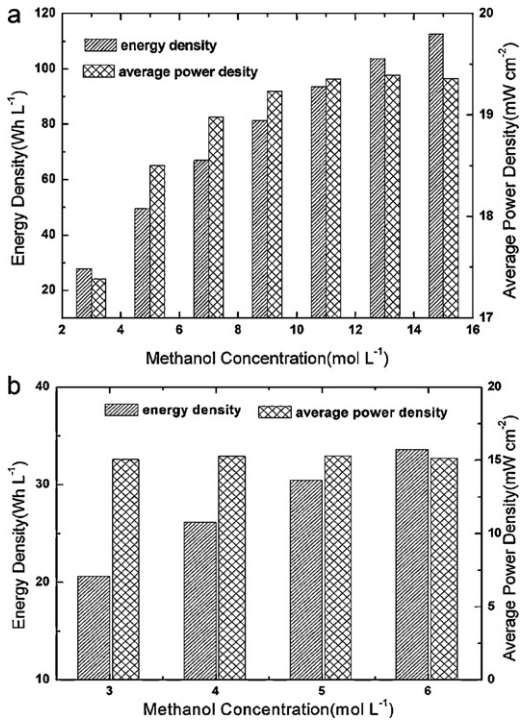

Fig. 11. Calculated energy densities and average output power densities of the (a) LE-DMFC and (b) C-DMFC with various methanol concentrations.

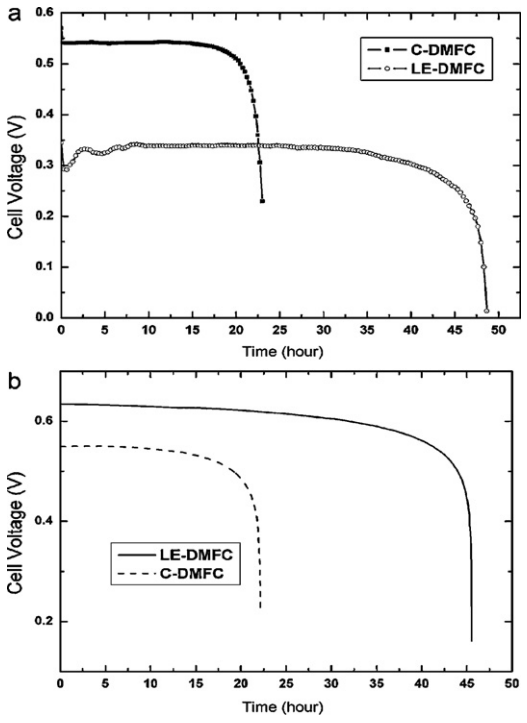

Fig. 12. (a) Experimental; (b) calculated discharging data for LE-DMFC and C-DMFC at 2.5 mA cm^{-2} with 1.0 mol L^{-1} methanol solution.

5. Conclusions

In this work, a specially designed passive LE-DMFC with a composite electrolyte was fabricated to reduce methanol crossover. The composite electrolyte had two Nafion-112 membranes with a 0.2 cm LE layer in the middle. A corresponding mathematical model was also proposed to optimize the cell parameters and working conditions. The LE-DMFC with a composite electrolyte performed much better than the C-DMFC due to its lower methanol crossover flux. In particular, the LE-DMFC can be fed with highly concentrated methanol. The cell performance of the LE-DMFC was almost identical when fed with methanol solutions of 3.0 mol L^{-1} and 12.0 mol L^{-1}. The LE-DMFC with 15.0 mol L^{-1} methanol solution could work continuously for approximately 33 h, which was two times longer than the C-DMFC fed with 6.0 mol L^{-1} methanol solution. The highest energy density obtained from the C-DMFC was only approximately 30 Wh L^{-1}, whereas the energy density of the LE-DMFC reached 110 Wh L^{-1}. By employing an LE layer, the fuel utilization of the LE-DMFC was improved by more than 100%, which was affirmed by both the experimental and calculated discharging data.

Acknowledgements

This work was supported by the National Natural Science Foundation of China (20876153, 20703043, 21073180, 20933004, and 21011130027), the Science & Technology Research Programs of Jilin Province (20102204), and the High Technology Research Program (863 program, 2007AA05Z159 and 2007AA05Z143) of the Science and Technology Ministry of China.

References

[1] K.M. McGrath, G.K.S. Prakash, G.A. Olah, J. Ind. Eng. Chem. 10 (2004) 1063–1080.
[2] A. Heinzel, V.M. Barragan, J. Power Sources 84 (1999) 70–74.
[3] S.N. Xue, G.P. Yin, Polymer 47 (2006) 5044–5049.
[4] J. Saito, K. Miyatake, M. Watanabe, Macromolecules 41 (2008) 2415–2420.
[5] D. Yamamoto, H. Munakata, K. Kanamura, J. Electrochem. Soc. 155 (2008) B303–B308.
[6] Y.S. Choi, T.K. Kim, E.A. Kim, S.H. Joo, C. Pak, Y.H. Lee, H. Chang, D. Seung, Adv. Mater. 20 (2008) 2341–2344.
[7] H.W. Zhang, X.H. Fan, J. Zhang, Z.T. Zhou, Solid State Ionics 179 (2008) 1409–1412.
[8] P.X. Xing, G.P. Robertson, M.D. Guiver, S.D. Mikhailenko, K.P. Wang, S. Kaliaguine, J. Membr. Sci. 229 (2004) 95–106.
[9] S. Reichman, L. Burstein, E. Peled, J. Power Sources 179 (2008) 520–531.
[10] Y.M. Kim, K.W. Park, J.H. Choi, I.S. Park, Y.E. Sung, Electrochem. Commun. 5 (2003) 571–574.
[11] Z.Q. Ma, P. Cheng, T.S. Zhao, J. Membr. Sci. 215 (2003) 327–336.
[12] Z.G. Shao, X. Wang, I.M. Hsing, J. Membr. Sci. 210 (2002) 147–153.
[13] M.A. Smit, A.L. Ocampo, M.A. Espinosa-Medina, P.J. Sebastian, J. Power Sources 124 (2003) 59–64.
[14] V. Tricoli, F. Nannetti, Electrochim. Acta 48 (2003) 2625–2633.
[15] P. Dimitrova, K.A. Friedrich, U. Stimming, B. Vogt, Solid State Ionics 150 (2002) 115–122.
[16] D.H. Jung, S.Y. Cho, D.H. Peck, D.R. Shin, J.S. Kim, J. Power Sources 118 (2003) 205–211.
[17] K. Kordesch, V. Hacker, U. Bachhiesl, Proceedings of the 22nd International Power Sources Symposium, Elsevier Science Sa, Manchester, England, 2001, pp. 200–203.
[18] T. Schaffer, V. Hacker, J.O. Besenhard, Meeting of the International-Battery-Association (IBA), Elsevier Science Bv, Graz, Austria, 2004, pp. 217–227.
[19] E. Kjeang, J. Goldak, M.R. Golriz, J. Gu, D. James, K. Kordesch, Fuel Cells 5 (2005) 486–498.
[20] E. Kjeang, J. Goldak, M.R. Golriz, J. Gu, D. James, K. Kordesch, J. Power Sources 153 (2006) 89–99.
[21] K.D. Kreuer, S.J. Paddison, E. Spohr, M. Schuster, Chem. Rev. 104 (2004) 4637–4678.
[22] H. Bahrami, A. Faghri, J. Power Sources 196 (2011) 1191–1204.
[23] R.E. Delarue, C.W. Tobias, J. Electrochem. Soc. 106 (1959) 827–833.
[24] K. Scott, W. Taama, J. Cruickshank, J. Power Sources 65 (1997) 159–171.
[25] A.A. Kulikovsky, Electrochem. Commun. 4 (2002) 939–946.
[26] H. Guo, C.F. Ma, Electrochem. Commun. 6 (2004) 306–312.